Formononetin may protect aged hearts from ischemia/reperfusion damage by enhancing autophagic degradation

ZHENGXIN HUANG[1*], YINGFENG LIU[1*] and XIANPING HUANG[2]

[1]Department of Cardiology, Zhujiang Hospital, Southern Medical University, Guangzhou, Guangdong 510000; [2]Laboratory of Biochemistry, Hunan University of Chinese Medicine, Changsha, Hunan 410000, P.R. China

Received December 28, 2017; Accepted May 1, 2018

DOI: 10.3892/mmr.2018.9544

Abstract. Myocardial infarction is a leading cause of mortality worldwide, and timely blood/oxygen reperfusion may substantially improve the outcome of infarction. However, ischemia/reperfusion (I/R) may cause severe side effects through excess reactive oxygen species generation. To develop novel methods to relieve I/R induced cell damage, the present study used a component of traditional Chinese medicine. In the present study, isolated heart tissue from aged mice and H9C2 cells with chemically-induced aging were used as experimental subjects, and it was demonstrated that formononetin was able to alleviate I/R-induced cell or tissue apoptosis. By applying formononetin to I/R-damaged tissue or cells, it was demonstrated that formononetin was able to enhance autophagy and thus alleviate I/R-induced cell damage. Furthermore, it was observed that I/R was able to inhibit lysosomal degradation processes in aged tissues or cells by impairing the lysosome acidification level, and formononetin was able to reverse this process via the re-acidification of lysosomes. In conclusion, the present study demonstrated that formononetin was able to alleviate I/R-induced cellular apoptosis in aged cells by facilitating autophagy.

Introduction

Myocardial infarction is a leading cause of mortality worldwide, and timely blood/oxygen reperfusion using either thrombolytic therapy or primary percutaneous coronary intervention may efficiently limit the myocardial infarct size, preserve left ventricular systolic function and reduce the onset of heart failure (1). However, immediate reperfusion may produce a large amount of reactive oxygen species (ROS), subsequently inducing myocardial cell apoptosis and finally causing severe ischemia/reperfusion (I/R) cardiac injury (2). At present, efforts are being made to relieve ROS-induced myocardial cell damage. Among those efforts, emerging evidence suggests that the modulation of autophagy may be a novel therapeutic strategy for myocardial I/R injury (3).

Autophagy is a degradative process used to eliminate long-lived proteins and damaged organelles. Autophagy involves multiple steps, including the generation of autophagosomes, fusion of autophagosomes and lysosomes, and protein degradation in lysosomes (4). Previous research has demonstrated that autophagy dysfunction may lead to numerous health issues, including neurodegeneration, cardiomyopathy, cancer and I/R injury (4-7). It is widely accepted that increased autophagic flux may protect the cell from I/R injury, as autophagy eliminates impaired organelles and thus limits the spread of damage inside the cell. I/R preconditioning is one of the best-researched and commonly used methods of relieving I/R injury. It has been demonstrated that I/R preconditioning may protect heart cells through pre-activation of autophagy (8,9). However, in a recent *in vivo* animal study, researchers demonstrated that in heart tissues from aged rats, preconditioning was unable to induce autophagic activity efficiently, which finally led to more severe heart I/R injury in aged rats (10).

Traditional Chinese medicines, including *Radix Astragali*, have been widely used to treat cardiovascular disease (11). As a principal isoflavone compound extracted from *Radix Astragali*, formononetin has been reported to have numerous pharmacological properties, including anticancer, anti-inflammatory, antioxidant, antiviral and neuroprotective activity, and wound healing (12-14). However, the molecular mechanisms underlying the cardioprotective potential of formononetin within the context of myocardial infarction and subsequent I/R injury remain unclear. Considering that autophagy has been proven to protect myocardial cell from I/R injury, the present study raised the hypothesis that formononetin may protect aged myocardial cells from I/R damage by regulating autophagy.

Materials and methods

Reagents. Dulbecco's modified Eagle's medium (DMEM), fetal bovine serum (FBS), and penicillin/streptomycin (10,000 U/ml

Correspondence to: Dr Zhengxin Huang, Department of Cardiology, Zhujiang Hospital, Southern Medical University, 253 Gongyedadao Road, Guangzhou, Guangdong 510000, P.R. China
E-mail: hda20161@yeah.net

*Contributed equally

Key words: ischemia/reperfusion, aging cells, autophagy, formononetin, Chinese traditional medicine

each) were purchased from Gibco (Thermo Fisher Scientific, Inc., Waltham, MA, USA). Dimethyl sulfoxide and berberine were obtained from Sigma-Aldrich (Merck KGaA, Darmstadt, Germany). The rabbit monoclonal antibody against β-actin (cat. no. ab8227) was obtained from Abcam (Cambridge, UK). Anti-Caspase-3 (cat. no. 9662), cytochrome *c* (Cyt-c; cat. no. 12963), apoptosis regulator Bcl-2 (Bcl-2; cat. no. 15071), Beclin-1 (cat. no. 3738), autophagy protein 5 (Atg-5; cat. no. 2630) and p62 (cat. no. 23214) antibodies were purchased from Cell Signaling Technology, Inc. (Danvers, MA, USA). Horseradish peroxidase (HRP)-conjugated goat anti-rabbit secondary antibodies (cat. no. A-21109) used in western blotting were obtained from Invitrogen (Thermo Fisher Scientific, Inc.).

Plasmids. EGFP-LC3b (cat. no. 11546) and pLV-mCherry (cat. no. 36084) were obtained from Addgene, Inc. (Cambridge, MA, USA). To construct the mCherry-GFP-LC3 plasmid, PCR was performed for mCherry from the pLV-mCherry vector with a pair of primers (Forward, 5'-GCTAGCGCC TGGAGCTGCTTGGCCACCATGCCCCAGACTGTGAGT TGC-3' and reverse, 5'-GCTAGCATAAAGACACCAAG GAAGCTGACAAGATAGAGGAAGAGCAA-3') containing the *Nhe*1 target sequence, 21 random nucleotides in between as linker and a 21 nucleotide matching mCherry sequence. PCR was performed with PfuUltra High-Fidelity DNA polymerase (Agilent Technologies, USA). dNTPs were purchased from New England Biolabs, Inc. (Ipswich, MA, USA). The following thermocycling conditions were used: 94˚C 5 min, followed by 30 cycles of 94˚C for 30 sec, 55˚C for 30 sec and 72˚C for 1 min, with a final extension at 72˚C for 10 min. The PCR product was subjected to *Nhe*1 digestion at 37˚C overnight (New England Biolabs, Inc.) and gel extraction. The *Nhe*1 site between the CMV promoter and EGFP in EGFP-LC3b vector was also digested by *Nhe*1 for 1 h at 37˚C, followed by CIP (calf alkaline phosphatase; New England Biolabs, Inc.) treatment for 1 h at 37˚C (New England Biolabs, Inc.). Following gel extraction, both vector and PCR inserts were ligated with T4-ligase (New England Biolabs, Inc.).

Isolated heart preparation. Aged male mice (n=60; 10 months old; 35-45 g) were used for the present study. All animal experiments were conducted in compliance with the Guide for the Care and Use of Laboratory Animals published by the National Institutes of Health, and were approved by the Animal Care Committees of Southern Medical University (Guangzhou, China). Mice were obtained from the Experimental Animal Center of Southern Medical University (ID: 2015030856). All mice were housed in plastic cages at 25˚C and 50±5% relative humidity under a 12 h light/dark cycle with free access to rodent chow and water. They were housed for one week to adapt to their environment prior to experimentation. Mice were anesthetized with 2% pentobarbital sodium (50 mg/kg intraperitoneally), and the hearts were mounted in a Langendorff perfusion apparatus and subjected to simulated I/R as described previously (15). The Krebs-Henseleit buffer (KH buffer; 118 mM NaCl, 4.7 mM KCl, 1.2 mM $MgSO_4$, 1.25 mM $CaCl_2$, 1.2 mM KH_2PO_4, 25 mM $NaHCO_3$ and 11 mM glucose; pH 7.4) was equilibrated with 95% O_2 and 5% CO_2 at 37˚C for 30 min. The coronary flow rate was maintained at 6 ml/min during the stabilization, with a constant pressure of 80 mm H_2O throughout the experiment.

Experimental protocols. Each heart was stabilized for 20 min. Following stabilization, isolated hearts were divided into four groups, and each group included 10 hearts (n=10). In the control group, after 20 min stabilization, the heart was directly perfused with KH buffer for 100 min. In the I/R group (I/R), following stabilization, the hearts were exposed to 40 min ischemia followed by 60 min reperfusion. In the I/R+preconditioning group (I/R+PC), following stabilization, the hearts were exposed to ischemia for 40 min and then subjected to an I/R cycle including 10 sec reperfusion and 10 sec simulated ischemia, repeated six times. Hearts were subsequently reperfused for 60 min. In the I/R+formononetin group (I/R+Form), following stabilization, the hearts were exposed to ischemia for 40 min, and 5 mM formononetin was administered at the onset of reperfusion for 10 sec. This protocol was repeated a further five times and followed by 60 min reperfusion.

Evaluation of myocardial infarct size. At the end of reperfusion, all hearts were rapidly frozen for 1.5 h at -20˚C and subsequently cut into six transverse slices (~3 mm thick) parallel to the atrioventricular groove. Then each slice was incubated for 15 min in a 1% solution of triphenyltetrazolium chloride (TTC) in phosphate buffer at 37˚C. This method is used to reliably distinguish the necrotic myocardium (which appears pale) from the viable myocardium that stains brick-red. The extent of the area of necrosis was quantified by computerized planimetry with ImageJ software (version 1.50i; National Institutes of Health, Bethesda, MD, USA), correcting for the weight of the tissue slices. The total weight of the area of necrosis was calculated and expressed as a percentage of the total left ventricular weight.

Cardiac function. A catheter was inserted into the left ventricle of the mice through the left atrium as described previously (16). The left ventricular end-diastolic pressure was adjusted to 5-7 mm Hg during the initial equilibrium phase. The distal end of the catheter was connected to a Power Lab 8/SP™ data acquisition system (ADInstruments, Dunedin, New Zealand) via a pressure transducer for the continuous recording of cardiac function. Cardiac function was evaluated based on left ventricular developed pressure. Fractional shortening (FS) was calculated as follows: FS = [left ventricular end diastolic diameter (LVEDD)-left ventricular end systolic diameter (LVESD)]/LVEDD x100. The ejection fraction (EF) was calculated from left ventricular end-diastolic volume (LVEDV) and end-systolic volume (LVESD) using the equation (LVEDV-LVESV)/LVEDV x100.

Measurement of apoptosis by terminal deoxynucleotidyl-transferase-mediated dUTP nick end labeling (TUNEL) assay in myocardial tissues. At the end of reperfusion, the left ventricle free wall was collected and sliced into 1-mm^2 sections from each group. Myocardial sections were fixed with 10% formalin for 48 h at room temperature, and subsequently sliced into 4-5 μm sections, as described previously (17). The apoptotic myocytes were stained via

a TUNEL assay using a TUNEL kit (Beyotime Institute of Biotechnology, Beijing, China) according to the manufacturer's instructions. Nuclei were stained with 0.5 μg/ml DAPI in glycerol mounting buffer (Beyotime Biotechnology) at room temperature for 1 h. A total of three sections from each myocardial sample were randomly selected, and 10 microscopic fields per section were evaluated by single photon confocal microscopy (x10 objective lens; Olympus Corporation, Tokyo, Japan). The apoptotic index was determined by dividing the cell number of TUNEL-positive nuclei by the total number of cells and multiplying by 100.

Hypoxia/reoxygenation (H/R) model of D-galactose-induced aging in H9C2 cells. The D-galactose induction was conducted as previously described (18). D-galactose (10 g/l) was added to H9C2 cells for 48 h at 37˚C. Hypoxic conditions were produced using D-Hank's solution (Beyotime Institute of Biotechnology) saturated with 95% N_2 and 5% CO_2 at 37˚C. The pH was regulated to 6.8 using lactate to mimic ischemic conditions. Aged H9C2 cells were put into a hypoxic incubator which was equilibrated with 1% O_2, 5% CO_2 and 94% N_2 at 37˚C. Following the hypoxia period, the culture medium was rapidly replaced with fresh DMEM with 10% FBS (normoxic culture solution) to mimic reoxygenation.

Cell viability assay. Cell viability was measured using a Cell Counting Kit-8 (CCK-8, BiYunTian, Beijing, China). Cells were seeded in 96-well plates at a concentration of $3x10^3$ cells/well. After 24 h of each treatment as described above (Control, I/R, I/R+PC and I/R+Form), 10 μl of CCK-8 was immediately added to each well. Subsequently, cells were incubated for 2 h at 37˚C. Using a microplate spectrophotometer, the plates were read at 570 nm to determine their optical density.

Please add a subsection containing the full protocol for western blotting, including the following details:

Western blotting. Total proteins were extracted from heart tissues or aged cells. Samples were lysed with radioimmunoprecipitation assay buffer (1% NP-40, 0.5% sodium deoxycholate, 0.1% SDS, 150 mM NaCl, 1 mM EDTA, and 50 mM Tris-HCl; pH 7.4) with a protease inhibitor cocktail (Sigma-Aldrich; Merck KGaA) and centrifuged at 12,000 x g for 10 min at 4˚C. Protein concentrations in supernatants were measured with a bicinchoninic acid protein assay(BiYunTian, Beijing, China). Protein samples (50 μg/lane) were separated by 12% SDS-PAGE and subsequently transferred onto polyvinylidene fluoride membranes. Membranes were blocked in 5% bovine serum albumin (Sigma-Aldrich; Merck KGaA) with Tris-buffered saline with 1% Tween-20 for 1 h at room temperature and then incubated overnight at 4˚C with primary antibodies against Caspase-3, Cyt-c, Bcl-2, Beclin-1, Atg-5, p62 and β-actin (all 1:2,000; Cell Signaling Technology, Inc.). Following this, membranes were incubated with HRP-conjugated goat anti-rabbit secondary antibodies (1:5,000, Abcam, China) for 1 h at room temperature. Target bands were visualized by enhanced chemiluminescence (BiYunTian, Beijing, China). The density of specific bands was analyzed using with ImageJ software (version 1.50i; National Institutes of Health) and normalized to β-actin.

Plasmids transfection and live cell imaging. H9C2 cells were transfected for 24 h with different constructs using Lipofectamine® 2000 (Invitrogen; Thermo Fisher Scientific, Inc.) according to the manufacturer's instructions. Live cell images for H9C2 cells were captured by a single photon confocal microscopy (x60 objective lens; Olympus Corporation). LysoTracker-Red staining was observed 5 min subsequent to reagent administration at 37˚C. The colocalization of different vesicles or the number of single vesicles was quantified using ImageJ software (version 1.50i, National Institutes of Health, Bethesda, MD, USA) with Coloc 2 plugin (version 2.1.0; imagej.net/Coloc_2). A two-tailed, two-sample, unequal variance Student's t-test was used to calculate the P-values. Error bars represent the standard deviation of the samples.

Statistical analysis. All data are expressed as the mean ± standard deviation and represent at least three independent experiments. Statistical comparisons were performed using SPSS 11.0 (SPSS, Inc., Chicago, IL, USA). using a Student's t-test or one-way analysis of variance followed by a post hoc analysis (Tukey's test) where applicable. $P<0.05$ was considered to indicate a statistically significant difference.

Results

Pretreatment with formononetin reduces myocardial tissue injury, improves cardiac function and decreases apoptosis in heart tissue. As hypothesized, the results of the present study demonstrated that I/R treatment induced extensive infarct injury (pale tissue sections following TTC staining) compared with the control group. Notably, although preconditioning was unable to effectively rescue heart infarct injury, pretreatment with formononetin at 5 mM was able to significantly reduce the areas of the pale sections (Fig. 1A and B). The average infarct size was 46% in the I/R group and was reduced to 23% following pretreatment with formononetin. These data indicated that pretreatment with formononetin may relieve cardiac infarct injury in heart tissue from aged mice. To examine whether pretreatment with formononetin improved cardiac function following I/R injury, echocardiography was used to measure cardiac functional indices, including LVESD, LVEDD, FS and EF.

As presented in Fig. 1, LVESD in the I/R group increased to 4.14±0.75 mm compared with the control group (2.50±0.44 mm), and treatment with formononetin reduced this to 3.1±0.27 mm (Fig. 1C). Similarly, LVEDD was increased to 4.61±0.69 mm in the I/R group compared with 3.01±0.43 mm in the control group, and treatment with formononetin reduced this to 3.52±0.16 mm (Fig. 1D). These two measurements suggested that treatment with formononetin alleviated cardiac dilation following I/R injury. Furthermore, values of FS (16.16±5.31%) and EF (29.29±6.97%) in the I/R group were reduced when compared with the control group (33.22±3.56% and 66.07±9.15%, respectively) and treatment with formononetin significantly increased these two indices (Fig. 1E and F). Therefore, treatment with formononetin reduced the size of infarct lesions and improved cardiac function in I/R-induced heart failure.

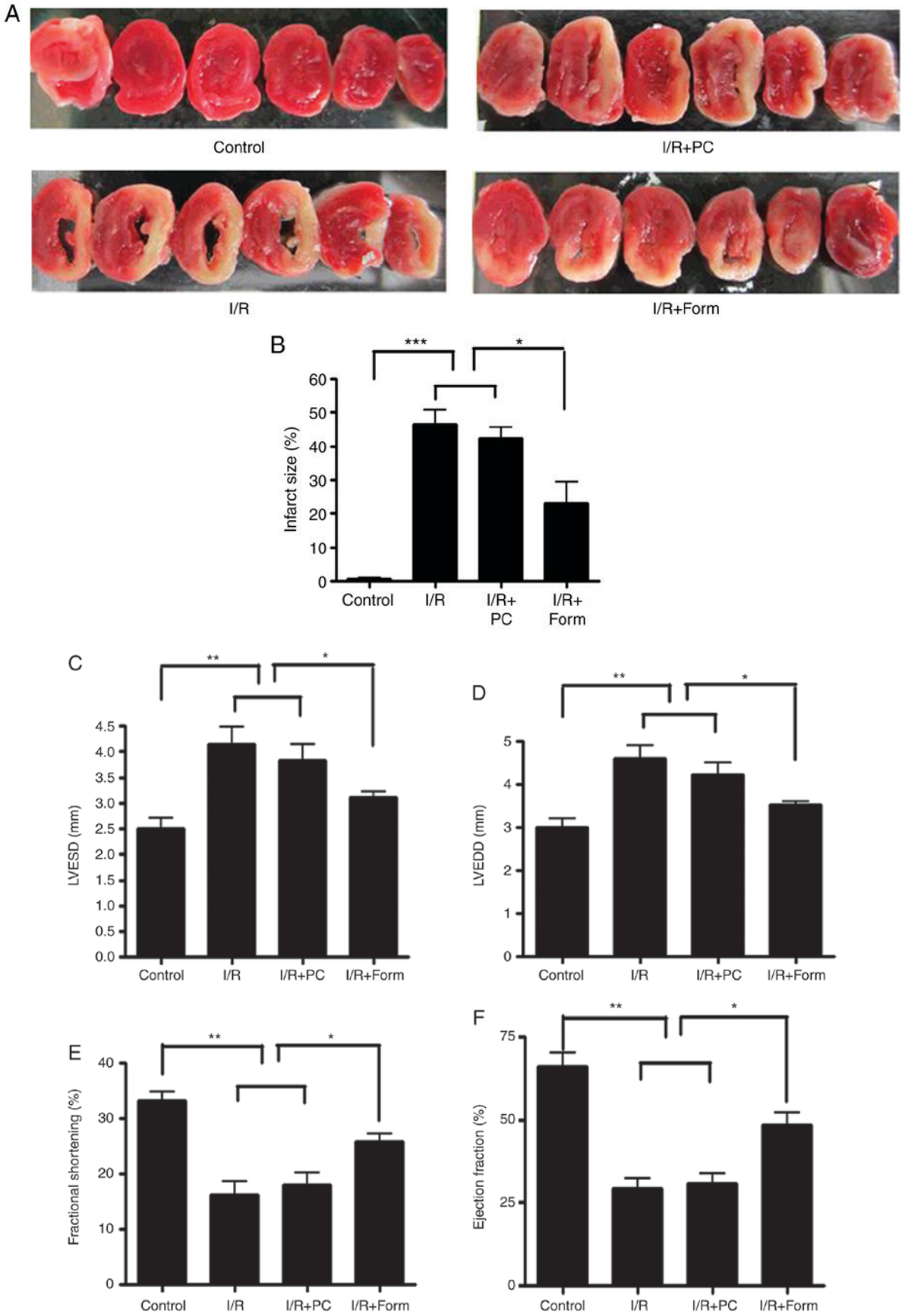

Figure 1. Pretreatment with formononetin reduces myocardial tissues injury, improves cardiac function and decreases apoptosis in heart tissue from aged mice. (A) Infarct size was measured using triphenyltetrazolium chloride staining to distinguish necrotic from viable myocardium. White zones indicate infarcted sections. (B) Infarct size (expressed as the percentage risk zone of the total left ventricle). The effects of various interventions on hemodynamic parameters in the isolated aged mice hearts were assessed: (C) left ventricular end systolic diameter; (D) left ventricular end diastolic diameter ; (E) fractional shortening; and (F) ejection fraction. The data are from four independent experiments. *P<0.05, **P<0.01 and ***P<0.001. I/R, ischemia/reperfusion; Form, treated with formononetin; PC, preconditioning.

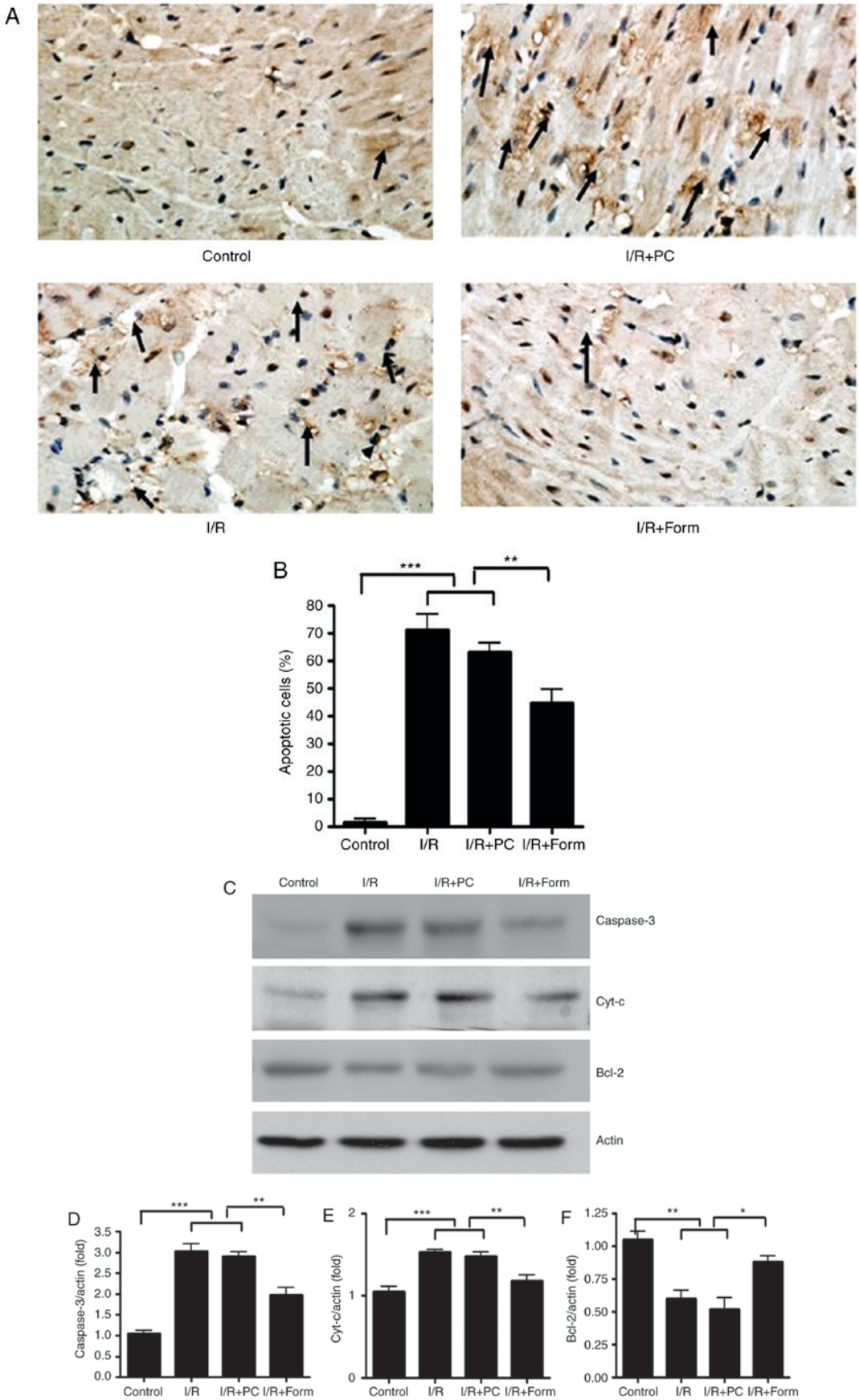

Figure 2. Formononetin rescues I/R-induced cellular apoptosis in isolated heart tissue. (A) TUNEL staining detected cardiomyocyte apoptosis. Nuclei with brown staining indicate TUNEL-positive cells. Arrows indicate apoptotic cells (x400 magnification). (B) Statistical analysis of the results of the TUNEL assay. (C) Western blot analysis of cleaved caspase-3 (19 kDa), Cyt-c (14 kDa) and Bcl-2 (26 kDa). The intensity of each band was quantified and normalized to actin: (D) caspase 3; (E) Cyt-c; and (F) Bcl-2. All data were from three independent experiments. *P<0.05, **P<0.01 and ***P<0.001. TUNEL, terminal deoxynucleotidyl-transferase-mediated dUTP nick end labeling; I/R, ischemia/reperfusion; Form, treated with formononetin; PC, preconditioning; Cyt-c, cytochrome *c*; Bcl-2, apoptosis regulator Bcl-2.

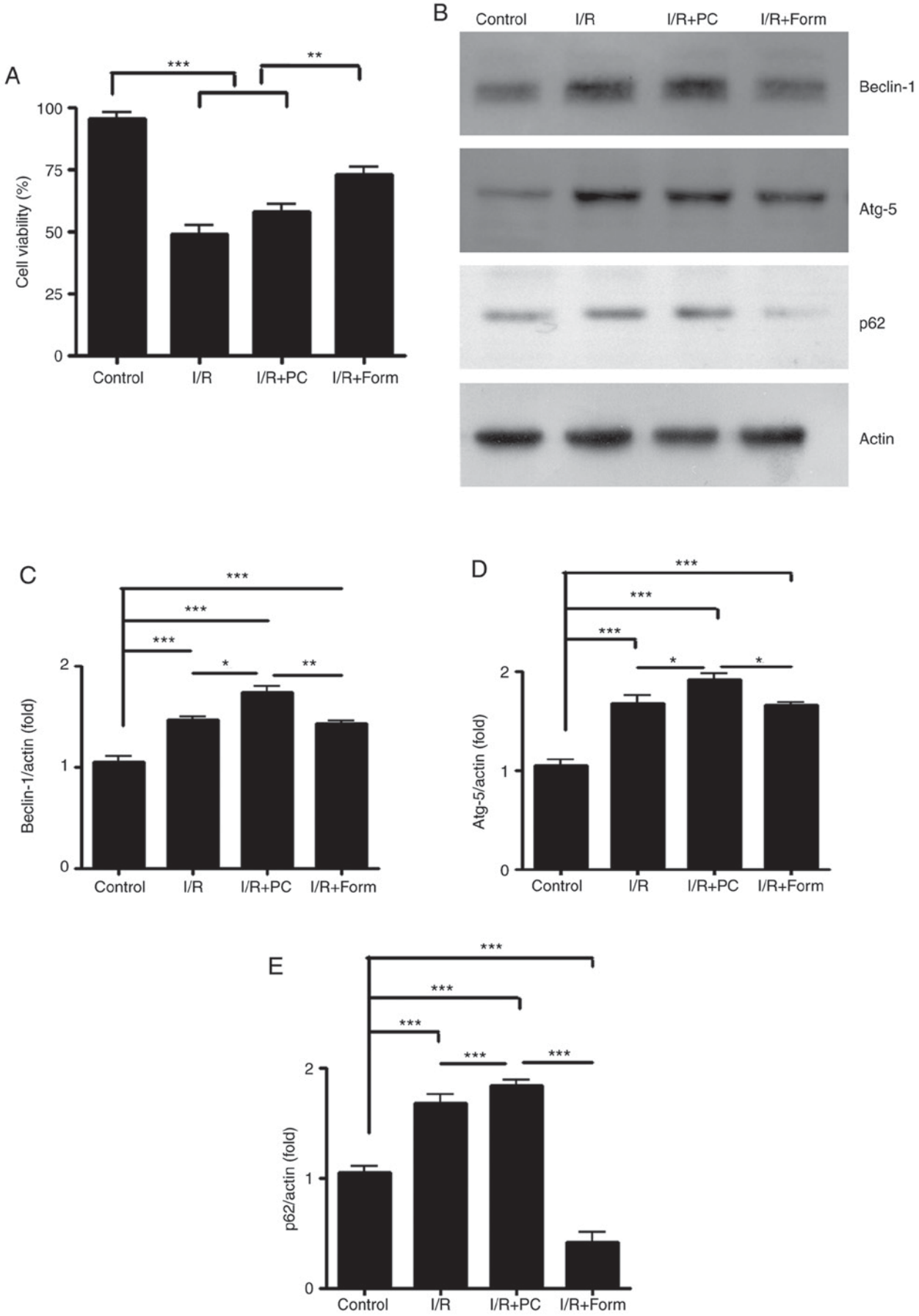

Figure 3. Formononetin alleviates I/R-induced cellular apoptosis in aged H9C2 cells by enhancing cellular autophagy. (A) The cell viability of H9C2 cells following the indicated treatments. (B) Western blot analysis of Beclin-1 (60 kDa), Atg-5 (55 kDa) and p62 (62 kDa). The intensity of each band was quantified and normalized to actin: (C) Beclin-1; (D) Atg-5; and (E) p64. All data were from three independent experiments. *P<0.05, **P<0.01 and ***P<0.001. I/R, ischemia/reperfusion; Form, treated with formononetin; PC, preconditioning; Atg-5, autophagy protein 5.

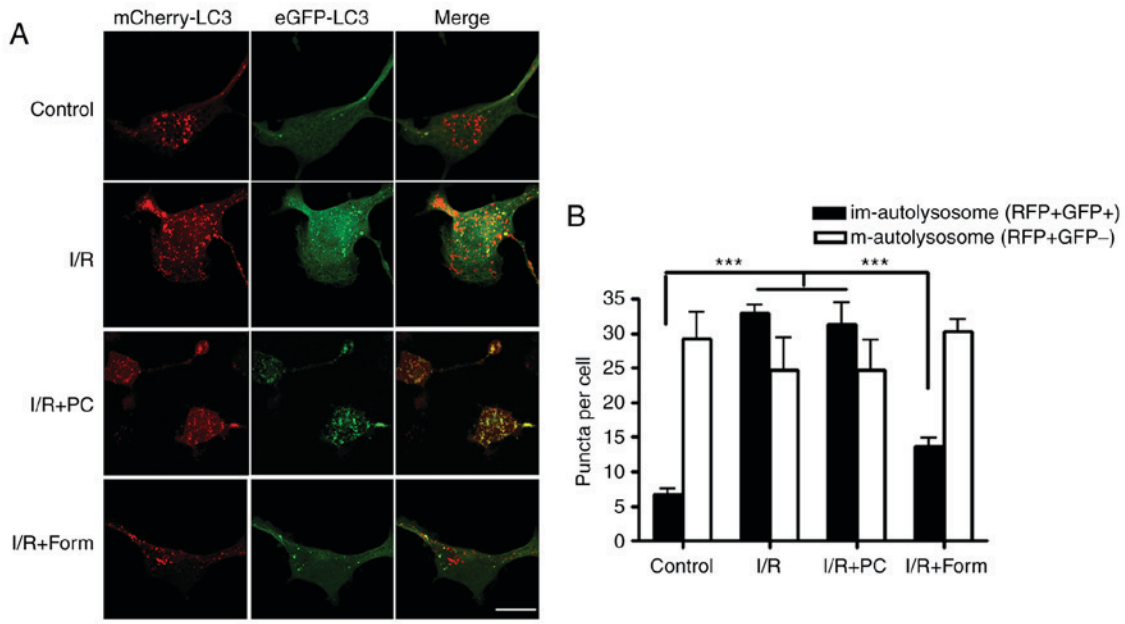

Figure 4. Formononetin regulates autolysosome maturation. (A) H9C2 cells were transfected with an eGFP-mCherry-LC3 tandem construct under the indicated conditions. (B) Numbers of immature autophagosomes (GFP^+RFP^+) and mature autolysosomes (GFP^-RFP^+) were counted under each condition. Scale bar, 10 μm. n=10. ***P<0.001. I/R, ischemia/reperfusion; Form, treated with formononetin; PC, preconditioning; eGFP, enhanced green fluorescent protein; LC3, microtubule-associated proteins 1A/1B light chain 3; im, immature; m, mature.

Formononetin rescues I/R-induced cellular apoptosis in isolated heart tissue. The present study investigated apoptosis markers in isolated hearts from aged mice. The data in Fig. 2 demonstrate that following I/R injury, the number of apoptotic cells was significantly increased in the I/R group, and treatment with formononetin was able to reduce this number (Fig. 2A and B). Furthermore, western blot analysis demonstrated that following I/R or I/R with PC, the density of cleaved caspase-3 and Cyt-c was significantly increased, while that of Bcl-2 was decreased. This result additionally indicated that preconditioning was unable to effectively rescue I/R-induced cellular apoptosis in the aged heart. However, it was identified that pretreatment with formononetin reversed the alterations in all of the above markers, which indicated that formononetin may protect the aged heart from I/R injury through a mechanism different from that of preconditioning.

Formononetin alleviates I/R-induced cellular apoptosis in aged H9C2 cells. To further investigate the detailed mechanism underlying the cardioprotective effects of formononetin, a chemically-induced aging H9C2 cell line was used in the present study. Similar to the isolated hearts, a marked apoptosis phenotype was observed in aged H9C2 cells by CCK-8 assay (Fig. 3A) in both I/R and I/R+PC groups. This result indicated that the *in vitro* chemically-induced aging H9C2 cells were able to be used to mimic I/R injury. The present study subsequently assessed whether formononetin administration to aged H9C2 cells alleviated I/R-induced apoptosis. The results in Fig. 3 demonstrated that formononetin decreased the cellular apoptosis rate following I/R injury.

Formononetin enhances cellular autophagic activity in aged H9C2 cells. As autophagy is an important mechanism for cell survival following I/R injury, the present study sought to investigate whether autophagy was involved in the I/R model. Through western blotting, it was observed that in aged H9C2 cells, I/R increased the expression of Beclin-1 and Atg5, two well-known autophagy indicators. Furthermore, preconditioning elevated the Beclin-1 and Atg5 expression levels to a greater extent. However, compared with preconditioning, formononetin led to a more modest elevation of Beclin-1 and Atg5 protein expression (Fig. 3B-D). p62, an autophagy degradation marker, was detected and it was observed that although I/R and preconditioning increased Beclin-1 and Atg5 efficiently, they failed to decrease p62 expression compared with the control or formononetin groups (Fig. 3E). This result indicated that although I/R and PC initiated the autophagy process in aged H9C2 cells, they did not lead to its completion due to unknown reasons. By contrast, although formononetin increased Beclin-1 expression modestly, it was able to effectively decrease p62 expression following I/R injury.

To further investigate how autophagy is involved in I/R-induced cellular apoptosis, mCherry-EGFP-LC3B was used. As GFP and mCherry have different pKa values, GFP does not exhibit fluorescence in an environment with a pH <4.5; however, mCherry may fluoresce in an environment with a pH as low as 1.0. Determined by the different physical characteristics of mCherry and GFP, a green vesicle was taken to indicate a newly-formed autophagosome, a red vesicle indicated a mature autolysosome and a yellow vesicle indicated an immature autolysosome. By transfecting this construct into aged cells, it was identified that there were more yellow vesicles in the I/R and I/R+PC groups. However, pretreatment with formononetin was able to decrease the number of yellow autolysosomes and increase the number of mature autolysosomes (Fig. 4). These results indicated that I/R led to a greater number of immature autolysosomes in aged H9C2 cells, while pretreatment with formononetin rescued this phenotype.

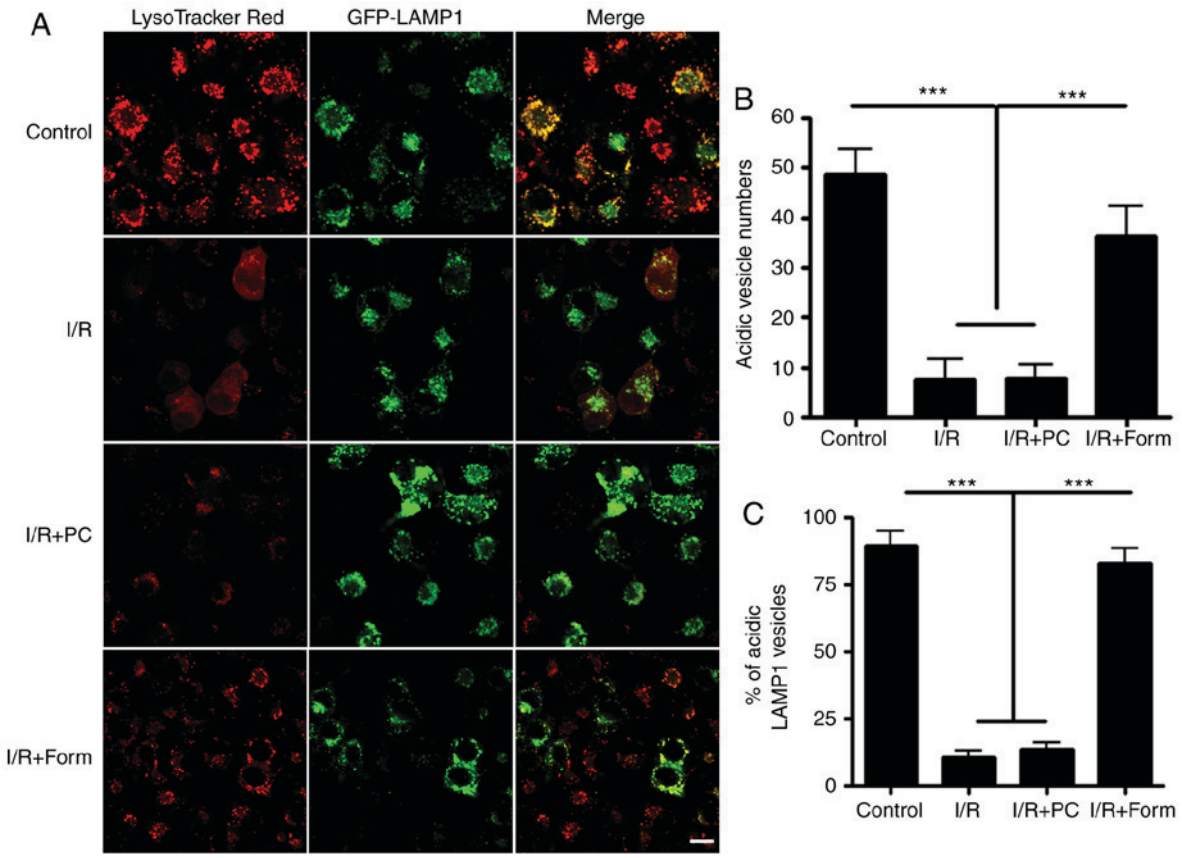

Figure 5. Formononetin regulates autolysosome acidification levels. (A) H9C2 cells were treated with LysoTracker and transfected with GFP-LAMP1. (B) Numbers of acidic vesicles (red) were counted under each of the indicated conditions. (C) Colocalization of acidic vesicles (red) with lysosomes (GFP) was calculated. Scale bar, 20 μm. n=10. ***P<0.001. I/R, ischemia/reperfusion; Form, treated with formononetin; PC, preconditioning; eGFP, enhanced green fluorescent protein; LAMP1, lysosome-associated membrane glycoprotein 1.

Formononetin regulates autophagy by modulating lysosomal acidification. To further investigate the mechanisms underlying how formononetin regulated autophagy, the cells were treated with LysoTracker Red, an acidic vesicle indicator. By co-transfecting with GFP-lysosome-associated membrane glycoprotein 1, a lysosome indicator, it was observed that the majority of lysosomes were colocalized with LysoTracker in the control group. However, following I/R injury, there was a significantly decreased number of acidic vesicles in the aged cells. Finally, it was identified that formononetin was able to restore the number of acidic vesicles compared with the I/R or I/R + PC groups (Fig. 5).

Discussion

Myocardial infarction is the irreversible death of heart cells caused by a prolonged period of oxygen deprivation. A total of ~1.5 million cases of myocardial infarction occur annually in the USA (19). Immediate oxygen recovery is the most efficient way to treat an infarction. However, the excess of ROS generated following reperfusion may cause severe side effects, including heart cell apoptosis (20-23). Therefore, either enhancing endogenous ROS elimination pathways or applying exogenous medication to inhibit ROS production have become the most promising methods of avoiding I/R injury.

Autophagy is an endogenous protein degradation pathway involving the process of autophagosome generation, fusion with lysosomes and eventual lysosome degradation. Physiologically, autophagy may degrade incorrectly folded proteins or eliminate damaged organelles, and this is an important step in preventing any potential cytotoxicity or stress inside the cell, and subsequently preventing cellular apoptosis. Due to the natural functions of autophagy, methods that are able to evoke autophagic activity efficiently have attracted increasing research interest. Since the autophagic process comprises a number of key steps, arresting at any of these may cause the autophagic process to be incomplete. In the present study, it was demonstrated that although autophagy was evoked efficiently in aging cells in the I/R+PC group, the protein clearance inside the autophagosome was blocked in aged cells following I/R injury.

Recent studies have reported controversial results on elevated autophagic activity and I/R injury. Certain studies have demonstrated that autophagy is critical to the elimination of I/R-induced ROS (24,25), while other reports have demonstrated that excess autophagic activity may aggravate cellular apoptosis (26,27). The differences between previous reports may come from different cell types, experimental designs or research methods. For example, although certain studies have counted GFP-LC3 dots as autophagic activity, this marker may only indicate the stimulation of autophagy, and not a complete autophagic clearance process. In the present study, GFP-mCherry LC-3 constructs were used to indicate autophagosomes and autolysosomes. Combined with

p62 protein level detection and LysoTracker live staining results, it was observed that following I/R injury, degradation inside the autolysosome/lysosome was blocked in aged cells. The results of the present study indicated there were a number of 'non-functional' autolysosomes/lysosomes in the aged cells, which may be considered to be an excess of autophagy if inappropriate observation methods are used.

Since the ability of aged cells to maintain metabolic homeostasis is frequently diminished, it was hypothesized that I/R may cause more severe injury in aged cells. Notably, by treating the aged cells with hypoxia preconditioning, a well established model for cell to evoke autophagy and adapt I/R condition, the present study demonstrated that cell viability was not markedly restored, which indicated that autophagy may not be involved in the response of aged cells to I/R injury. However, upon investigation of the mechanisms, it was demonstrated that the acidic level of lysosomes in aged cells was impaired by I/R injury. Thus, lysosome degradation impairment may be considered as the reason.

Formononetin is a principal isoflavone compound extracted from *Radix Astragali*, which has long been used to treat cardiovascular diseases in traditional Chinese medicine. For example, formononetin has been reported to be able to reduce intracellular ROS by inhibiting mitogen activated protein kinase 8 phosphorylation (28); to inhibit breast cancer cell proliferation by regulating the phosphatidylinositol 3-kinase (PI3K)/RAC-α serine/threonine-protein kinase (AKT)/serine/threonine-protein kinase mTOR signaling pathway (29); to increase adipocyte thermogenesis by modulating peroxisome proliferator-activated receptor-γ activity (30); or to have neuroprotective effects following traumatic brain injury by increasing microRNA-155 and heme oxygenase-1 expression (31). Regarding I/R injury, formononetin has been reported to markedly reduce the infarct volume and brain water accumulation in a rat model of I/R injury via activation of the PI3K/Akt signaling pathway (32). In the present study, it was additionally observed that formononetin was able to alleviate I/R-induced cellular apoptosis in aged isolated hearts or aged H9C2 cells. Sulfonated formononetin additionally exhibits cardioprotective effects in acute myocardial infarction in rats, possibly by regulating energy metabolism in cardiac mitochondria (33). Apart from the aforementioned literature, the present study is the first, to the best of our knowledge, to demonstrate that formononetin may protect aged heart cells from I/R injury by modulating autophagic activity.

Although the detailed mechanisms remain largely unknown, the results of the present study demonstrated that formononetin was able to restore the lysosome acidic level. H^+ concentrations inside lysosome are largely controlled by the vascular-type ATPase (v-ATPase) protein channel, and a recent study reported that formononetin was able to phosphorylate glycogen synthase kinase-3β (GSK-3B) at the Ser-9 site in a concentration-dependent manner (34). Considering that GSK-3B may regulate some members of v-ATPase family (35), it may be hypothesized that formononetin may modulate lysosome acidic level by regulating GSK-3B activity. In conclusion, the present study demonstrated that formononetin was able to regulate lysosome H^+ concentrations in aged cells following I/R injury, and thus evoke autophagy and protect cells from I/R injury.

Acknowledgements

Not applicable.

Funding

No funding was received.

Availability of data and materials

The datasets used and/or analyzed during the present study are available from the corresponding author on reasonable request.

Authors' contributions

ZH analyzed the data and wrote the manuscript. XH and YL performed the experiments and collected the data.

Ethics approval and consent to participate

All animal experiments were conducted in compliance with the Guide for the Care and Use of Laboratory Animals published by the National Institutes of Health, and were approved by the Animal Care Committees of Southern Medical University (Guangzhou, China).

Patient consent for publication

Not applicable.

Competing interests

The authors declare that they have no competing interests.

References

1. Showkathali R and Natarajan A: Antiplatelet and antithrombin strategies in acute coronary syndrome: State-of-the-art review. Curr Cardiol Rev 8: 239-249, 2012.
2. Wei Y, Ruan L, Zhou G, Zhao L, Qi B, Ouyang P, Jin Z, Zhang C and Liu S: Local ischemic postconditioning during primary percutaneous coronary intervention: A meta-analysis. Cardiology 123: 225-233, 2012.
3. Liu J, Wu P, Wang Y, Du Y, A N, Liu S, Zhang Y, Zhou N, Xu Z and Yang Z: Ad-HGF improves the cardiac remodeling of rat following myocardial infarction by upregulating autophagy and necroptosis and inhibiting apoptosis. Am J Transl Res 8: 4605-4627, 2016.
4. MS, Q Li and Y Liu. Autophagy and Alzheimer's Disease. Cellular and molecular neurobiology, 1-12.
5. Sun M, Asghar SZ and Zhang H: The polarity protein Par3 regulates APP trafficking and processing through the endocytic adaptor protein Numb. Neurobiol Dis 93: 1-11, 2016.
6. Cortese A, Tucci A, Piccolo G, Galimberti CA, Fratta P, Marchioni E, Grampa G, Cereda C, Grieco G, Ricca I, *et al*: Novel CLN3 mutation causing autophagic vacuolar myopathy. Neurology 82: 2072-2076, 2014.
7. Song H, Yan C, Tian X, Zhu N, Li Y, Liu D, Liu Y, Liu M, Peng C, Zhang Q, *et al*: CREG protects from myocardial ischemia/reperfusion injury by regulating myocardialautophagy and apoptosis. Biochim Biophys Acta 1863: 1893-1903, 2017.
8. Yi J, He G, Yang J, Luo Z, Yang X and Luo X: Heat acclimation regulates the autophagy-lysosome function to protect against heat stroke-induced brain injury in mice. Cell Physiol Biochem 41: 101-114, 2017.

9. Wu CL, Chen CH, Hwang CS, Chen SD, Hwang WC and Yang DI: Roles of p62 in BDNF-dependent autophagy suppression and neuroprotection against mitochondrial dysfunction in rat cortical neurons. J Neurochem 140: 845-861, 2017.
10. Chen J, Gao J, Sun W, Li L, Wang Y, Bai S, Li X, Wang R, Wu L, Li H and Xu C: Involvement of exogenous H2S in recovery of cardioprotection from ischemic post-conditioning via increase of autophagy in the aged hearts. Int J Cardiol 220: 681-692, 2016.
11. Wang HL, Zhou QH, Xu MB, Zhou XL and Zheng GQ: Astragaloside IV for experimental focal cerebral ischemia: Preclinical evidence and possible mechanisms. Oxid Med Cell Longev 2017: 8424326, 2017.
12. Tian Z, Liu SB, Wang YC, Li XQ, Zheng LH and Zhao MG: Neuroprotective effects of formononetin against NMDA-induced apoptosis in cortical neurons. Phytother Res 27: 1770-1775, 2013.
13. Li Q and Sun M: Effects of potassium ion channels in term pregnant myometrium. J Obstet Gynaecol Res 38: 479; author reply 480-481, 2012.
14. Zhou R, Xu L, Ye M, Liao M, Du H and Chen H: Formononetin inhibits migration and invasion of MDA-MB-231 and 4T1 breast cancer cells by suppressing MMP-2 and MMP-9 through PI3K/AKT signaling pathways. Horm Metab Res 46: 753-760, 2014.
15. Li H, Wang Y, Wei C, Bai S, Zhao Y, Li H, Wu B, Wang R, Wu L and Xu C: Mediation of exogenous hydrogen sulfide in recovery of ischemic post-conditioning-induced cardioprotection via down-regulating oxidative stress and up-regulating PI3K/Akt/GSK-3β pathway in isolated aging rat hearts, Cell Biosci 5: 11, 2015.
16. Liu Y, Ye Z, Luo H, Sun M, Li M, Fan D and Chui D: Inhalative formaldehyde exposure enhances aggressive behavior and disturbs monoamines in frontal cortex synaptosome of male rats. Neurosci Lett 464: 113-116, 2009.
17. Canene-Adams K: Preparation of formalin-fixed paraffin-embedded tissue for immunohistochemistry. Methods Enzymol 533: 225-233, 2013.
18. Yue Z, Rong J, Ping W, Bing Y, Xin Y, Feng LD and Yaping W: Gene expression of the p16(INK4a)-Rb and p19(Arf)-p53-p21(Cip/Waf1) signaling pathways in the regulation of hematopoietic stem cell aging by ginsenoside Rg1. Genet Mol Res 13: 10086-10096, 2014.
19. Benjamin EJ, Blaha MJ, Chiuve SE, Cushman M, Das SR, Deo R, de Ferranti SD, Floyd J, Fornage M, Gillespie C, *et al*: Heart disease and stroke statistics-2017 update: A report from the American Heart Association. Circulation 135: e146-e603, 2017.
20. Yu Y, Zhou L, Sun M, Zhou T, Zhong K, Wang H, Liu Y, Liu X, Xiao R, Ge J, *et al*: Xylocoside G reduces amyloid-β induced neurotoxicity by inhibiting NF-κB signaling pathway in neuronal cells. J Alzheimers Dis 30: 263-275, 2012.
21. Yu J, Sun M, Chen Z, Lu J, Liu Y, Zhou L, Xu X, Fan D and Chui D: Magnesium modulates amyloid-beta protein precursor trafficking and processing. J Alzheimers Dis 20: 1091-1106, 2010.
22. Wang H, Sun M, Yang H, Tian X, Tong Y, Zhou T, Zhang T, Fu Y, Guo X, Fan D, *et al*: Hypoxia inducible factor 1α mediates up regulation of neprilysin by histone deacetylase1 under hypoxia condition in neuroblastoma cells. J Neurochem 131: 4-11, 2014.
23. Ding W, Cai Y, Wang W, Ji L, Dong Y, Zhang X, Su M, Liu J, Lu G and Zhang X: Adiponectin protects the kidney against chronic intermittent hypoxia-induced injury through inhibiting endoplasmic reticulum stress. Sleep Breath 20: 1069-1074, 2016.
24. Fan T, Chen L, Huang Z, Wang W, Zhang B, Xu Y, Mao Z, Hu H and Geng Q: Autophagy activation by rapamycin before hypoxia-reoxygenation reduces endoplasmic reticulum stress in alveolar epithelial cells. Cell Physiol Biochem 41: 79-90, 2017.
25. Ning Y, Li Z and Qiu Z: FOXO1 silence aggravates oxidative stress-promoted apoptosis in cardiomyocytes by reducing autophagy. J Toxicol Sci 40: 637-645, 2015.
26. Xia Y, Liu Y, Xia T, Li X, Huo C, Jia X, Wang L, Xu R, Wang N, Zhang M, *et al*: Activation of volume-sensitive Cl-channel mediates autophagy-related cell death in myocardial ischaemia/reperfusion injury. Oncotarget 7: 39345-39362, 2016.
27. Huang Z, Han Z, Ye B, Dai Z, Shan P, Lu Z, Dai K, Wang C and Huang W: Berberine alleviates cardiac ischemia/reperfusion injury by inhibiting excessive autophagy cardiomyocytes. Eur J Pharmacol 762: 1-10, 2015.
28. Lee H, Lee D, Kang KS, Song JH and Choi YK: Inhibition of intracellular ROS accumulation by formononetin attenuates cisplatin-mediated apoptosis in LLC-PK1 cells. Int J Mol Sci 19: E813, 2018.
29. Zhou R, Chen H, Chen J, Chen X, Wen Y and Xu L: Extract from Astragalus membranaceus inhibit breast cancer cells proliferation via PI3K/AKT/mTOR signaling pathway. BMC Complement Altern Med 18: 83, 2018.
30. Nie T, Zhao S, Mao L, Yang Y, Sun W, Lin X, Liu S, Li K, Sun Y, Li P, *et al*: A natural compound, formononetin, extracted from astragalus membranaceus increase adipocyte thermogenesis by modulating PPARγ activity. Br J Pharmacol 175: 1439-1450, 2018.
31. Li Z, Wang Y, Zeng G, Zheng X, Wang W, Ling Y, Tang H and Zhang J: Increased miR-155 and heme oxygenase-1 expression is involved in the protective effects of formononetin in traumatic brain injury in rats. Am J Transl Res 9: 5653-5661, 2017.
32. Liang K, Ye Y, Wang Y, Zhang J and Li C: Formononetin mediates neuroprotection against cerebral ischemia/reperfusion in rats via downregulation of the Bax/Bcl-2 ratio and upregulation PI3K/Akt signaling pathway. J Neurol Sci 344: 100-104, 2014.
33. Zhang S, Tang X, Tian J, Li C, Zhang G, Jiang W and Zhang Z: Cardioprotective effect of sulphonated formononetin on acute myocardial infarction in rats. Basic Clin Pharmacol Toxicol 108: 390-395, 2011.
34. Cheng Y, Xia Z, Han Y and Rong J: Plant natural product formononetin protects rat cardiomyocyte H9c2 cells against oxygen glucose deprivation and reoxygenation via inhibiting ROS formation and promoting GSK-3β phosphorylation. Oxid Med Cell Longev 2016: 2060874, 2016.
35. Avrahami L, Farfara D, Shaham-Kol M, Vassar R, Frenkel D and Eldar-Finkelman H: Inhibition of glycogen synthase kinase-3 ameliorates β-amyloid pathology and restores lysosomal acidification and mammalian target of rapamycin activity in the Alzheimer disease mouse model: In vivo and in vitro studies. J Biol Chem 288: 1295-1306, 2013.